

## Polarization gating of high harmonic generation in the water window

Jie Li, Xiaoming Ren, Yanchun Yin, Yan Cheng, Eric Cunningham, Yi Wu, and Zenghu Chang

Citation: [Applied Physics Letters](#) **108**, 231102 (2016); doi: 10.1063/1.4953402

View online: <http://dx.doi.org/10.1063/1.4953402>

View Table of Contents: <http://scitation.aip.org/content/aip/journal/apl/108/23?ver=pdfcov>

Published by the [AIP Publishing](#)

---

### Articles you may be interested in

[Broadband second harmonic generation in GaAs nanowires by femtosecond laser sources](#)

*Appl. Phys. Lett.* **103**, 143110 (2013); 10.1063/1.4824024

[Nuclear signatures on the molecular harmonic emission and the attosecond pulse generation](#)

*J. Chem. Phys.* **136**, 054102 (2012); 10.1063/1.3681165

[Demonstration of extreme ultraviolet supercontinuum at the high harmonic plateau with a 6.5 fs/800 nm driving laser pulse](#)

*Appl. Phys. Lett.* **95**, 141102 (2009); 10.1063/1.3242361

[Effects of laser pulse duration on extreme ultraviolet spectra from double optical gating](#)

*Appl. Phys. Lett.* **93**, 111105 (2008); 10.1063/1.2982589

[High harmonic generation spectra of aligned benzene in circular polarized laser field](#)

*J. Chem. Phys.* **118**, 8726 (2003); 10.1063/1.1566737

---

The advertisement features a blue background with a molecular structure of a crystal lattice. On the left, there is a thumbnail image of an 'Applied Physics Reviews' journal cover. The main text reads 'NEW Special Topic Sections' in large white letters. Below this, it says 'NOW ONLINE' in yellow, followed by 'Lithium Niobate Properties and Applications: Reviews of Emerging Trends' in white. The AIP Applied Physics Reviews logo is in the bottom right corner.

**NEW Special Topic Sections**

**NOW ONLINE**  
Lithium Niobate Properties and Applications:  
Reviews of Emerging Trends

**AIP** Applied Physics Reviews

## Polarization gating of high harmonic generation in the water window

Jie Li, Xiaoming Ren, Yanchun Yin, Yan Cheng, Eric Cunningham, Yi Wu, and Zenghu Chang<sup>a)</sup>

*Institute for the Frontier of Attosecond Science and Technology, CREOL and Department of Physics, University of Central Florida, Orlando, Florida 32816, USA*

(Received 16 February 2016; accepted 25 May 2016; published online 6 June 2016)

We implement the polarization gating (PG) technique with a two-cycle, 1.7  $\mu\text{m}$  driving field to generate an attosecond supercontinuum extending to the water window spectral region. The ellipticity dependence of the high harmonic yield over a photon energy range much broader than previous work is measured and compared with a semi-classical model. When PG is applied, the carrier-envelope phase (CEP) is swept to study its influence on the continuum generation. PG with one-cycle (5.7 fs) and two-cycle (11.3 fs) delay are tested, and both give continuous spectra spanning from 50 to 450 eV under certain CEP values, strongly indicating the generation of isolated attosecond pulses in the water window region. *Published by AIP Publishing.* [<http://dx.doi.org/10.1063/1.4953402>]

Isolated attosecond laser sources achieved by high harmonic generation (HHG), since its first demonstration in 2001,<sup>1</sup> have opened a new window to understand electron dynamics and correlations.<sup>2</sup> These isolated attosecond pulses are normally generated using 800 nm driving lasers with various sub-cycle gating techniques,<sup>3</sup> such as amplitude gating (AG),<sup>4</sup> ionization gating,<sup>5</sup> polarization gating (PG),<sup>6,7</sup> double optical gating,<sup>8</sup> and attosecond lighthouses.<sup>9</sup> However, the cutoff photon energy of those isolated attosecond pulses driven by 800 nm lasers is limited to about 200 eV, which is one of the limitations of the shortest pulse duration that has been achieved thus far.<sup>10</sup> One of the challenges of attosecond science is to push the attosecond source's photon energy range into the water window (280–530 eV) for studying inner-shell electron dynamics in atoms, molecules, and condensed matter, as well as ultrafast processes in bio-specimens.

As has been demonstrated in 2001, the cutoff photon energy of HHG can be extended by increasing the wavelength of the driving laser.<sup>11</sup> With the recent flurry of development of mid-IR laser sources,<sup>12–16</sup> the HHG cutoff photon energy has reached the water window.<sup>17–20</sup> Proof of principal of several gating methods developed for 800 nm driving lasers have been demonstrated for 1.6–1.8  $\mu\text{m}$  lasers, although measurements of duration of isolated attosecond pulses in the water window are yet to be accomplished. Ishii *et al.* observed strong carrier-envelope-phase (CEP) dependence of the half-cycle cutoffs in the water window,<sup>19</sup> which is the foundation of AG, but single isolated attosecond pulses are only resultant in this case when the plateau harmonics are filtered out. Spatiotemporal isolation of attosecond pulses in the water window has been recently achieved by the attosecond lighthouse technique,<sup>21</sup> although few-cycle driving lasers are required, and the pointing direction of the attosecond beam is directly coupled to the CEP of the driving laser. Additionally, gating based on ionization and phase matching has been implemented for multi-cycle lasers,<sup>22</sup> but the intensity of the 2  $\mu\text{m}$  laser was kept low in order to precisely control the

ionization per laser cycle, so cutoff photon energy (200 eV) reached short of the carbon K-edge (280 eV).

Both AG and PG have played an important role for 800 nm driving lasers. It is known that a train of attosecond pulses are produced even when the linearly polarized driving lasers last only two cycles.<sup>3</sup> The spectrum corresponding to each attosecond pulse is an extreme ultraviolet (XUV) supercontinuum, the coherent superposition of which results in a modulated spectrum in the plateau region, which is the origin of the high-order harmonics. However, the cutoff photon energy of one spectrum differs from one another because they are generated by electrons recolliding with the parent ion under different laser field amplitude. AG was designed to take advantage of this cutoff difference. The spectrum in the cutoff region becomes continuous when the CEP of the driving laser is chosen properly. In this case, the return energy of one recollision is larger than all others so that a spectral filter can be placed after the generation target to select this continuous cutoff region to obtain an isolated attosecond pulse, limiting the spectral bandwidth of the isolated attosecond pulses generated by the AG. PG is a temporal switch for generating broadband isolated attosecond pulses.<sup>3</sup> When the polarization gate width is shorter than the spacing between adjacent attosecond bursts, only one recollision event occurs. As a result, both the plateau and cutoff become continuous, not just the cutoff region as in the AG.<sup>23</sup> This is only true for two-cycle or longer driving lasers. AG becomes more effective as the driving laser approaches one half-optical-cycle. In that case, only one recollision dominates the microscopic photon emission process. Consequently, broadband isolated attosecond pulses are produced when the short trajectory is phase-matched. Unlike attosecond lighthouse, the pointing direction of the attosecond beam generated by PG is not affected by the CEP of the driving laser, which makes the latter more appealing to applications where pointing stability is critical. CEP is also important for PG since it affects the energy of the attosecond pulses, as well as the intensity ratio between the main pulse to the satellite pulses. In addition, PG is a critical component of double optical gating, which can be implemented to both few- and multi-cycle driving

<sup>a)</sup> Author to whom correspondence should be addressed. Electronic mail: Zenghu.Chang@ucf.edu

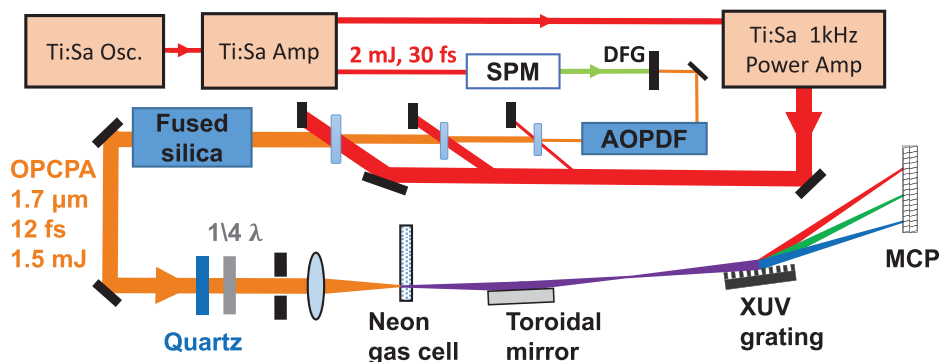


FIG. 1. Experimental setup for the OPCPA laser system and the HHG source. SPM: self-phase modulation; DFG: different frequency generation; and AOPDF: acousto-optic programmable dispersive filter for controlling spectral phase and CEP. The toroidal mirror is for future attosecond streaking experiments.

lasers.<sup>3</sup> Therefore, it is interesting to study the effectiveness of PG with long wavelength lasers. In this Letter, we demonstrate the experimental feasibility of generating isolated attosecond pulses using the PG technique with a CEP stabilized, two-cycle Optical Parametric Chirp Pulse Amplification (OPCPA) driving laser centered at  $1.7 \mu\text{m}$ . First, we measure the ellipticity-dependent HHG yield in the water window and compare the result with a semi-classical model. Based on the experiment, we design the PG scheme and demonstrate the feasibility of PG to generate soft x-ray supercontinua. The driving laser's CEP influence on the HHG spectrum is then studied to suggest the generation of isolated attosecond pulses in the water window.

The experiment (Fig. 1) is driven by a home-built 1 kHz OPCPA system.<sup>24</sup> The driving laser beam is loosely focused into a 1.5 mm-long gas cell filled with 1 bar neon pressure that was optimized for water window x-ray signals. The gas cell is located after the focus for phase matching the short trajectory. The material dispersion of the lens, entrance window and wave plates is pre-compensated by an Acousto-Optic Programmable Dispersive Filter (AOPDF), ensuring our driving pulse is near-transform-limited at the HHG gas cell. A 1200 line/mm laminar-type soft x-ray diffraction grating (Shimadzu 03-005) is chosen for an x-ray spectrometer that suppresses the high-order diffraction to observe high harmonics down to 50 eV where the resolution is sufficient to resolve harmonic peaks.<sup>25</sup> The grating is designed for covering 155–350 eV, and the diffraction efficiency falls rapidly above 350 eV.<sup>26</sup> The diffracted signal from 50 to 450 eV is collected simultaneously by a micro-channel plate detector with a phosphor screen, which is critical for studying the effects of PG on the plateau harmonics.

To study the ellipticity dependence of the HHG yield over a broad photon energy range that reaches the water window, an achromatic quarter-wave plate (Thorlabs AQWP10M-1600) is used to control the ellipticity of the driving field. The difference of the grating's efficiency with p- and s-polarization is neglected because the rotation of the major axis of the driving field ellipse is less than  $10^\circ$ , resulting in a relative error of only 3%. The laser peak intensity is estimated to be  $5 \times 10^{14} \text{ W/cm}^2$ , corresponding to a theoretical cutoff photon energy of 450 eV. Our measured result is shown in Fig. 2(a). In order to determine the ellipticity adequate for suppressing HHG at the edge of a polarization gate, we introduce the threshold ellipticity  $\varepsilon_{th}$ , defined as the point at which the harmonic yield drops by 90% (Fig. 2(b)). Because the ellipticity-dependent HHG yield follows a Gaussian shape in

theory,<sup>27</sup> a Gaussian fitting is used to determine the threshold ellipticity at different photon energies. We found the threshold ellipticity to be  $\varepsilon_{th} = 0.1$ , the dependence only slightly decreasing with the increase of x-ray photon energy. Compared to HHG driven by 800 nm lasers, which has a threshold ellipticity of  $\varepsilon_{th} = 0.2$ ,<sup>28</sup> the ellipticity dependence is much stronger, which indicates that PG is more effective for long wavelength driving laser. This is consistent with previous results where the cutoff photon energies are less than 200 eV.<sup>29,30</sup>

We use a semi-classical model to explain the dependence of HHG yield on ellipticity. This model assumes that

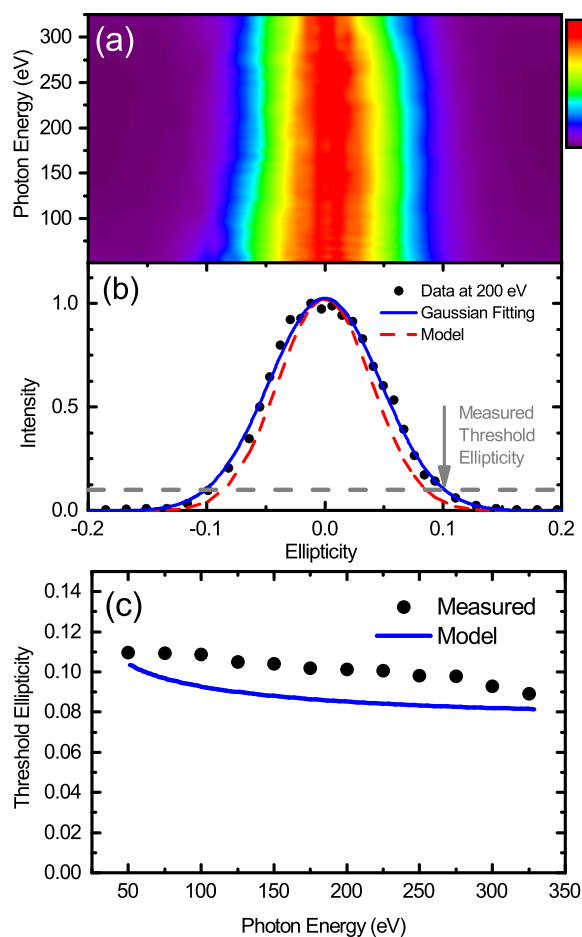


FIG. 2. (a) Dependence of HHG yield on the driving laser ellipticity over the range of 50–325 eV; (b) dependence of HHG yield on the driving laser ellipticity at 200 eV (dot) with its Gaussian fitting (solid line); and (c) measured (dot) and calculated (solid line) threshold ellipticity at a field intensity of  $5 \times 10^{14} \text{ W/cm}^2$ .

the XUV emission from an elliptical field is dominated by those electron trajectories whose transverse displacement caused by the field elliptical is compensated by an initial transverse velocity when the electron tunnels out of the atomic binding potential.<sup>28</sup> According to this model, the high harmonic intensity vs ellipticity curve is a mapping of the initial transverse velocity distribution of the electron freed from an atom via tunneling ionization. Here, we only show the modeling result in Figs. 2(b) and 2(c). The calculated threshold ellipticity matches the experimental data with an accuracy of better than 20% error.

In the PG experiment, the optical axis of a quartz plate of 180  $\mu\text{m}$  (379  $\mu\text{m}$ ) thickness is set at 45° with respect to the polarization of the linearly polarized input driving laser to introduce a one- (two-) cycle delay between the o- and e-pulses. The subsequent quarter-wave plate, with its optical axis set at 0°, converts the o- and e-pulses into counter-rotating circularly polarized pulses with a linearly polarized field in the overlap region.<sup>31,32</sup> The polarization gate width can be expressed as<sup>23</sup>

$$\delta t_G = \frac{\varepsilon_{th} \tau_p^2}{\ln(2) T_d}, \quad (1)$$

where  $\varepsilon_{th} = 0.1$  is the threshold ellipticity,  $\tau_p = 12$  fs is the pulse duration of our driving laser, and  $T_d = 5.6$  fs (11.3 fs) is the delay introduced by the one- (two-) cycle first quartz plate. The resulting polarization gate width is thus calculated to be  $\delta t_{G1} = 3.6$  fs ( $\delta t_{G2} = 1.8$  fs) for one- (two-) cycle delay. To choose the proper gate width appropriate for experiment, the polarization gate width should be less than half of one

optical cycle  $\delta t_G < T_0/2 = 2.8$  fs to ensure only a single recombination event occurs for each laser shot. Thus, it is apparent that the two-cycle delay PG satisfies this requirement, while the one-cycle delay PG will result in an incomplete gating.

We compare the HHG spectra using the linearly polarized driving pulse and the PG pulse under different CEP values (Fig. 3). Our laser intensity is estimated to be  $5.5 \times 10^{14}$  W/cm<sup>2</sup> for all cases. The HHG spectra under the linearly polarized driving field are always discrete regardless of the CEP value, indicating that multiple recombination events occur in the plateau spectrum region for each laser shot. For the incomplete gating ( $T_0/2 < \delta t_{G1} < T_0$ ) created by the one-cycle-delay PG, the form of the HHG spectra changes between comb-like (CEP = 0.45  $\pi$ ) and continuous (CEP = -0.05  $\pi$ ) due to multiple or single recombination events, respectively. For the complete gating ( $\delta t_{G2} < T_0/2$ ) created by the two-cycle-delay PG, the HHG spectra are always continuous for all CEP values, indicating that an isolated attosecond pulse is generated for each laser shot, as previously demonstrated with an 800 nm driving laser.<sup>7</sup> Another indication of isolated attosecond pulse generation is the large variation of the x-ray intensity with CEP in Figs. 3(c) and 3(f). The CE phase sets the timing between the center of the polarization gate and the maximum of the quasi-linearly polarized driving field that determines where the attosecond pulse is generated inside the polarization gate. Consequently, the attosecond pulse-generation efficiency depends strongly on CEP when the gate width is smaller than the temporal spacing between adjacent attosecond bursts.<sup>33</sup> The full HHG spectrum recorded from 50 to 450 eV

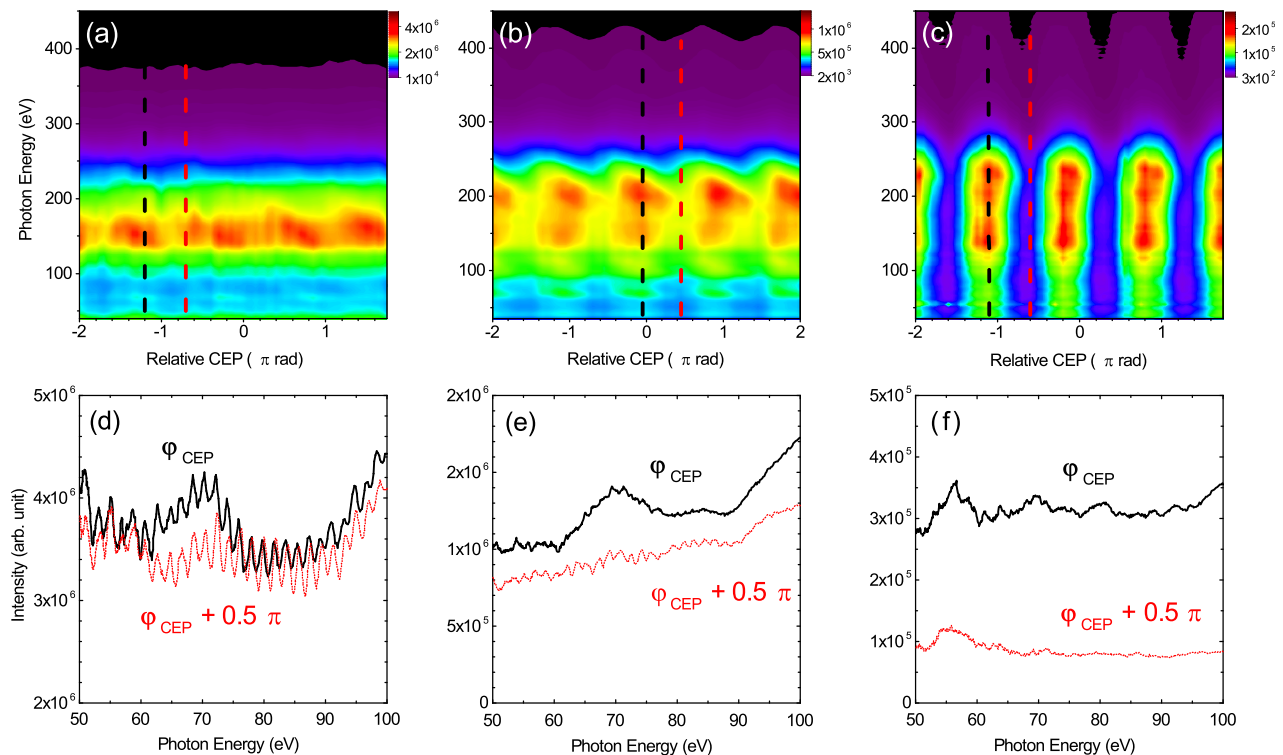


FIG. 3. CEP influence on HHG spectra using (a) a linear driving pulse, (b) a PG pulse with one-cycle delay, and (c) a PG pulse with two-cycle delay; comparison of HHG spectra with CEP values differing by 0.5  $\pi$  using (d) a linear driving pulse, (e) a PG pulse with one-cycle delay, and (f) a PG pulse with two-cycle delay. The spectra below 100 eV are shown where the resolution of spectrometer is sufficient to resolve harmonic peaks. The conditions of the MCP detector are kept the same so that the relative x-ray intensity in the three cases can be compared.

via the two-cycle-delay PG (CEP =  $-1.1 \pi$ ) is shown in Fig. 4. The HHG spectrum bandwidth supports a transform-limited attosecond pulse duration as short as 13 attosecond. It is known that attosecond pulses from the short trajectory are positively chirped. Compensating the atto-chirp with the negative group delay dispersion of thin Sn films or xenon gas is feasible in the 150–300 eV range, which may yield pulses less than 40 as shown in Ref. 34. Other materials such as Al and Zr can be used to compress pulses at lower photon energies in the broad plateau to meet different application requirements.<sup>3,34,35</sup> The number of x-ray photons in the 120–400 eV range was measured with an XUV photodiode (IRD AXUV100), which gives  $\sim 1.5 \times 10^7$  photons per laser shot after a 100 nm Sn filter, or  $\sim 3 \times 10^7$  before the filter. The filters were used to block the driving lasers. The measurement was done when the laser is linearly polarized laser so that it can be compared with the results reported in Ref. 20. The higher x-ray photon number in our measurements can be attributed to the higher driving laser energy available in this work.

In conclusion, we measured the ellipticity dependence of HHG yield in the water window using 1.7  $\mu\text{m}$ , 12 fs, CEP-stabilized laser pulses. The measured result agrees well with a semi-classical model. Compared to 800 nm driving lasers, the stronger ellipticity dependence makes PG more effective for the 1.7  $\mu\text{m}$  laser. A continuous HHG spectrum in the water window is demonstrated via the PG technique. The laser's CEP influence on the shape and intensity of the HHG spectrum strongly indicates isolated attosecond pulses are generated. The PG method demonstrated here is complementary to other grating schemes for long wavelength driving lasers. The continuous spectrum obtained with PG driven by 1.7  $\mu\text{m}$  lasers covers 50–450 eV, which is broader than the 75 eV bandwidth achieved with AG.<sup>19</sup> The cutoff photon energy, 400 eV, is higher than the 188 eV reached by ionization/phase matching gating.<sup>22</sup> The main advantage of the AG and ionization gating is the simplicity as no gating optics are required. It is expected that ultrabroad band light sources based on PG with mid-infrared lasers will play an important role in attosecond transient absorption experiments<sup>36,37</sup> to simultaneously observe electron motions in the core and

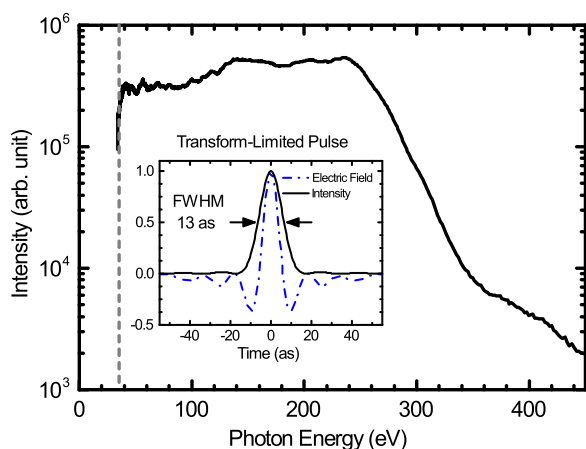


FIG. 4. HHG spectrum from via two-cycle-delay PG (CEP =  $-0.9 \pi$ ) with spectrum bandwidth supporting a transform-limited pulse duration of 13 as. Spectrum below 35 eV is clipped by the edge of our MCP detector.

valence levels. Characterization of the attosecond pulses generated by PG using the attosecond streaking camera technique is expected in the future.

This work has been supported by Army Researched Office under contact W1911NF-14-1-0383, Air Force Office of Scientific Research under contact FA9550-15-1-0037, the DARPA PULSE program by a grant from AMRDEC, and National Science Foundation.

- <sup>1</sup>M. Hentschel, R. Kienberger, Ch. Spielmann, G. A. Reider, N. Milosevic, T. Brabec, P. Corkum, U. Heinzmann, M. Drescher, and F. Krausz, *Nature* **414**, 509 (2001).
- <sup>2</sup>S. R. Leone, C. W. McCurdy, J. Burgdörfer, L. S. Cederbaum, Z. Chang, N. Dudovich, J. Feist, C. H. Greene, M. Ivanov, R. Kienberger, U. Keller, M. F. Kling, Z. Loh, T. Pfeifer, A. N. Pfeiffer, R. Santra, K. Schafer, A. Stolow, U. Thumm, and M. J. J. Vrakking, *Nat. Photonics* **8**(3), 162 (2014).
- <sup>3</sup>M. Chini, K. Zhao, and Z. Chang, *Nat. Photonics* **8**, 178 (2014).
- <sup>4</sup>E. Goulielmakis, M. Schultz, M. Hofstetter, V. S. Yakovlev, J. Gagnon, M. Uiberacker, A. L. Aquila, E. M. Gullikson, D. T. Attwood, R. Kienberger, F. Krausz, and U. Kleineberg, *Science* **320**, 1614 (2008).
- <sup>5</sup>A. Jullien, T. Pfeifer, M. J. Abel, P. M. Nagel, M. J. Bell, D. M. Neumark, and S. R. Leone, *Appl. Phys. B* **93**, 433 (2008).
- <sup>6</sup>P. B. Corkum, N. H. Burnett, and M. Y. Ivanov, *Opt. Lett.* **19**, 1870 (1994).
- <sup>7</sup>I. J. Sola, E. Mével, L. Elouga, E. Constant, V. Strelkov, L. Poletto, P. Villoresi, E. Benedetti, J.-P. Caumes, S. Stagira, C. Vozzi, G. Sansone, and M. Nisoli, *Nat. Phys.* **2**, 319 (2006).
- <sup>8</sup>H. Mashiko, S. Gilbertson, C. Li, S. D. Khan, M. M. Shakya, E. Moon, and Z. Chang, *Phys. Rev. Lett.* **100**, 103906 (2008).
- <sup>9</sup>K. T. Kim, C. Zhang, T. Ruchon, J. Hergott, T. Auguste, D. M. Villeneuve, P. B. Corkum, and F. Quéré, *Nat. Photonics* **7**, 651 (2013).
- <sup>10</sup>K. Zhao, Q. Zhang, M. Chini, Y. Wu, X. Wang, and Z. Chang, *Opt. Lett.* **37**, 3891 (2012).
- <sup>11</sup>B. Shan and Z. Chang, *Phys. Rev. A* **65**, 011804 (2001).
- <sup>12</sup>Y. Deng, A. Schwarz, H. Fattahi, M. Ueffing, X. Gu, M. Ossiander, T. Metzger, V. Pervak, H. Ishizuki, T. Taira, T. Kobayashi, G. Marcus, F. Krausz, R. Kienberger, and N. Karpowicz, *Opt. Lett.* **37**, 4973 (2012).
- <sup>13</sup>N. Ishii, K. Kaneshima, K. Kitano, T. Kanai, S. Watanabe, and J. Itatani, *Opt. Lett.* **37**, 4182 (2012).
- <sup>14</sup>B. E. Schmidt, A. D. Shiner, P. Lassonde, J. Kieffer, P. B. Corkum, D. M. Villeneuve, and F. Légaré, *and Opt. Express* **19**(7), 6858 (2011).
- <sup>15</sup>B. E. Schmidt, N. Thiré, M. Boivin, A. Laramée, F. Poitras, G. Lebrun, T. Ozaki, H. Ibrahim, and F. Légaré, *Nat. Commun.* **5**, 4643 (2014).
- <sup>16</sup>K. Hong, C. Lai, J. P. Siqueira, P. Krogen, J. Moses, C. Chang, G. J. Stein, L. E. Zapata, and F. X. Kärtner, *Opt. Lett.* **39**(11), 3145 (2014).
- <sup>17</sup>E. J. Takahashi, T. Kanai, K. L. Ishikawa, Y. Nabekawa, and K. Midorikawa, *Phys. Rev. Lett.* **101**, 253901 (2008).
- <sup>18</sup>M.-C. Chen, P. Arpin, T. Popmintchev, M. Gerrity, B. Zhang, M. Seaberg, D. Popmintchev, M. M. Murnane, and H. C. Kapteyn, *Phys. Rev. Lett.* **105**, 173901 (2010).
- <sup>19</sup>N. Ishii, K. Kaneshima, K. Kitano, T. Kanai, S. Watanabe, and J. Itatani, *Nat. Commun.* **5**, 3331 (2014).
- <sup>20</sup>S. L. Cousin, F. Silva, S. Teichmann, M. Hemmer, B. Buaes, and J. Biegert, *Opt. Lett.* **39**(18), 5383 (2014).
- <sup>21</sup>F. Silva, S. M. Teichmann, S. L. Cousin, M. Hemmer, and J. Biegert, *Nat. Commun.* **6**, 7611 (2015).
- <sup>22</sup>M.-C. Chen, C. Mancuso, C. Hernández-García, F. Dollara, B. Galloway, D. Popmintcheva, P.-C. Huang, B. Walker, L. Plajac, A. A. Jaron-Becker, A. Beckera, M. M. Murnane, H. C. Kapteyn, and T. Popmintcheva, *Proc. Natl. Acad. Sci.* **111**, E2361 (2014).
- <sup>23</sup>Z. Chang, *Phys. Rev. A* **70**, 043802 (2004).
- <sup>24</sup>Y. Yin, J. Li, X. Ren, K. Zhao, Y. Wu, E. Cunningham, and Z. Chang, *Opt. Lett.* **41**, 1142 (2016).
- <sup>25</sup>M. Koike, T. Namioka, E. M. Gullikson, Y. Harada, S. Ishikawa, T. Imazono, S. Mrowka, N. Miyata, M. Yanagihara, J. H. Underwood, K. Sano, T. Ogiwara, O. Yoda, and S. Nagai, *Proc. SPIE* **4146**, 163 (2000).
- <sup>26</sup>T. Imazono, M. Koike, T. Kawachi, N. Hasegawa, M. Koeda, T. Nagano, H. Sasaki, Y. Oue, Z. Yonezawa, S. Kuramoto, M. Terauchi, H. Takahashi, N. Handa, and T. Murano, *Proc. SPIE* **8848**, 884812 (2013).
- <sup>27</sup>M. Y. Ivanov, M. Spanner, and O. Smirnova, *J. Mod. Opt.* **52**, 165 (2005).

- <sup>28</sup>M. Möller, Y. Cheng, S. D. Khan, B. Zhao, K. Zhao, M. Chini, G. G. Paulus, and Z. Chang, *Phys. Rev. A* **86**, 011401 (2012).
- <sup>29</sup>H. Xu, H. Xiong, B. Zeng, W. Chu, Y. Fu, J. Yao, J. Chen, X. Liu, Y. Cheng, and Z. Xu, *Opt. Lett.* **35**, 472 (2010).
- <sup>30</sup>R. Cireasa, A. E. Boguslavskiy, B. Pons, M. C. H. Wong, D. Descamps, S. Petit, H. Ruf, N. Thiré, A. Ferré, J. Suarez, J. Higuete, B. E. Schmidt, A. F. Alharbi, F. Légraré, V. Blanchet, B. Fabre, S. Patchkovskii, O. Smirnova, Y. Mairesse, and V. R. Bhardwaj, *Nat. Phys.* **11**, 654 (2015).
- <sup>31</sup>O. Tcherbakoff, E. Mével, D. Descamps, J. Plumridge, and E. Constant, *Phys. Rev. A* **68**, 043804 (2003).
- <sup>32</sup>B. Shan, S. Ghimire, and Z. Chang, *J. Mod. Opt.* **52**, 277 (2005).
- <sup>33</sup>S. Gilbertson, S. D. Khan, Y. Wu, M. Chini, and Z. Chang, *Phys. Rev. Lett.* **105**, 093902 (2010).
- <sup>34</sup>D. H. Ko, K. T. Kim, and C. H. Nam, *J. Phys. B* **45**, 074015 (2012).
- <sup>35</sup>Z. Chang, *Phys. Rev. A* **71**, 023813 (2005).
- <sup>36</sup>E. Goulielmakis, Z.-H. Loh, A. Wirth, R. Santra, N. Rohringer, V. S. Yakovlev, S. Zherebtsov, T. Pfeifer, A. M. Azzeer, M. F. Kling, S. R. Leone, and F. Krausz, *Nature* **466**, 739 (2010).
- <sup>37</sup>H. Wang, M. Chini, S. Chen, C.-H. Zhang, F. He, Y. Cheng, Y. Wu, U. Thumm, and Z. Chang, *Phys. Rev. Lett.* **105**, 143002 (2010).